
Increasing the Interpretability of Recurrent Neural Networks Using Hidden Markov Models

Viktoriya Krakovna
Department of Statistics
Harvard University
vkrakovna@fas.harvard.edu

Finale Doshi-Velez
Department of Computer Science
Harvard University
finale@seas.harvard.edu

1 Introduction

Following the recent progress in deep learning, researchers and practitioners of machine learning are recognizing the importance of understanding and interpreting what goes on inside these black box models. Recurrent neural networks have recently revolutionized speech recognition and translation, and these powerful models would be very useful in other applications involving sequential data. However, adoption has been slow in applications such as health care, where practitioners are reluctant to let an opaque system make crucial decisions. If we can make the inner workings of RNNs more interpretable, more applications can benefit from their power.

A model or algorithm can be considered intelligible to humans in multiple ways, falling under the broad categories of transparency and post-hoc interpretability (Lipton, 2016). While works such as Ribeiro et al. (2016) and Turner (2016) develop post-hoc explanations for black-box models, we focus on transparency, specifically model parsimony and the ability to trace back from a prediction or model component to particularly influential features in the data, similarly to Kim et al. (2015).

This could be useful for understanding mistakes made by neural networks, which have human-level performance most of the time, but can perform very poorly on seemingly easy cases. For instance, convolutional networks can misclassify adversarial examples with very high confidence (Szegedy et al., 2014), and made headlines in 2015 when the image tagging algorithm in Google Photos mislabeled African Americans as gorillas. It's reasonable to expect recurrent networks to fail in similar ways as well. It would thus be useful to have more visibility into where these sorts of errors come from, i.e. which groups of features contribute to such flawed predictions.

Several promising approaches to interpreting RNNs have been developed recently, focusing on a state-of-the-art RNN architecture called Long Short-Term Memory (LSTM). Che et al. (2015) use gradient boosting trees to predict LSTM output probabilities and explain which features played a part in the prediction. They do not model the internal structure of the LSTM, but instead approximate the entire architecture as a black box. Karpathy et al. (2016) showed that in LSTM language models, around 10% of the memory state dimensions can be interpreted with the naked eye by color-coding the text data with the state values; some of them track quotes, brackets and other clearly identifiable aspects of the text. Building on these results, we take a somewhat more systematic approach to looking for interpretable hidden state dimensions, by using decision trees to predict individual hidden state dimensions (Figure 3). We visualize the overall dynamics of the LSTM hidden states by coloring the training data with the k-means clusters on the state vectors (Figure 2b).

We explore several methods for building more interpretable models by combining LSTMs and HMMs. The existing body of literature mostly focuses on methods that specifically train the RNN to predict HMM states (Bourlard and Morgan, 1994) or posteriors (Maas et al., 2012), referred to as hybrid or tandem methods respectively. We add the HMM state probabilities to the output layer of the LSTM, and then train the HMM and LSTM either sequentially or jointly (Figure 1). The LSTM model can make use of the information from the HMM, and fill in the gaps when the HMM is not performing well. This results in an LSTM with a smaller number of hidden state dimensions that

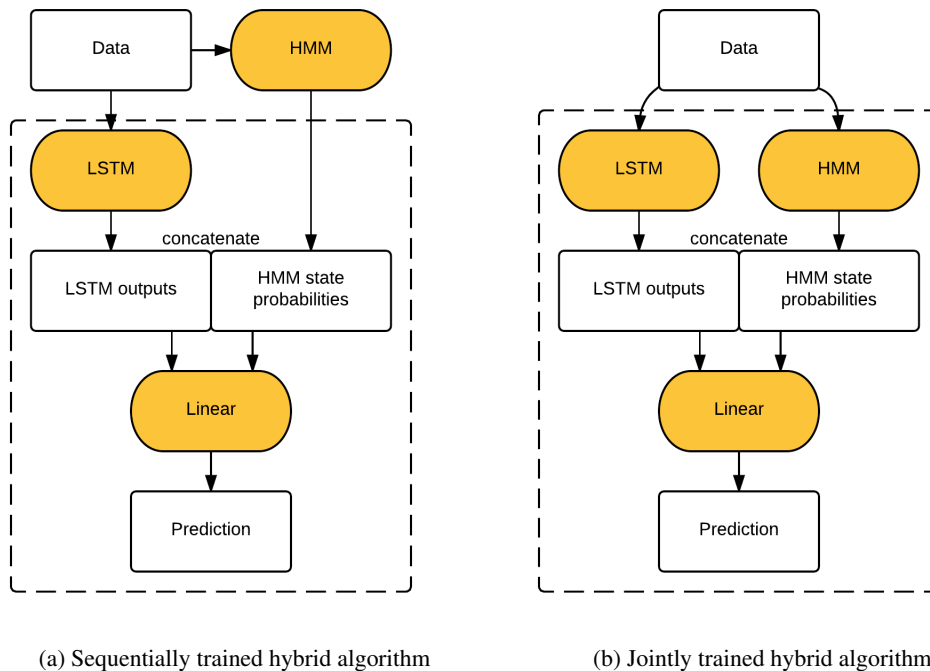


Figure 1: Hybrid HMM-LSTM algorithms (the dashed blocks indicate the components trained using SGD in Torch).

could be interpreted individually, especially for smaller data sets. We test the algorithms on text data and multivariate medical data.

2 Methods

2.1 LSTM

We use a character-level LSTM with 1 layer and no dropout, based on the Element-Research library. We train the LSTM for 10 epochs, starting with a learning rate of 1, where the learning rate is halved whenever $\exp(-l_t) > \exp(-l_{t-1}) + 1$, where l_t is the log likelihood score at epoch t . The L_2 -norm of the parameter gradient vector is clipped at a threshold of 5.

2.2 Hidden Markov models

We initialize the HMM hidden states as a random multinomial draw for each time step (i.i.d. across time steps). Then at each iteration:

1. Sample states using Forward Filtering Backwards Sampling algorithm (FFBS, Rao and Teh (2013)).
2. Sample transition parameters from a Multinomial-Dirichlet posterior with hyperparameter α . Let n_{ij} be the number of transitions from state i to state j . Then the posterior distribution of the i -th row of transition matrix T (corresponding to transitions from state i) is:

$$T_i \sim \text{Mult}(n_{ij}|T_i)\text{Dir}(T_i|\alpha)$$

3. Sample the emission parameters from a Multinomial-Dirichlet posterior.

2.3 Hybrid models

Our main hybrid model is put together sequentially, as shown in Figure 1a. We first run the discrete HMM on the data, outputting the hidden state distributions obtained by the HMM's forward pass,

Table 1: Predictive loglikelihood (LL) comparison, sorted by validation set performance.

(a) Linux text data				(b) Shakespeare text data			
Method	LSTM dim	HMM states	LL	Method	LSTM dim	HMM states	LL
HMM		10	-2.76	HMM		10	-2.69
HMM		20	-2.55	HMM		20	-2.5
LSTM	5		-2.54	LSTM	5		-2.41
Joint hybrid	5	10	-2.37	Hybrid	5	10	-2.3
Hybrid	5	10	-2.33	Hybrid	5	20	-2.26
Hybrid	5	20	-2.25	LSTM	10		-2.23
Joint hybrid	10	10	-2.19	Joint hybrid	5	10	-2.21
LSTM	10		-2.17	Hybrid	10	10	-2.19
Hybrid	10	10	-2.14	Hybrid	10	20	-2.16
Hybrid	10	20	-2.07	Joint hybrid	10	10	-2.12
LSTM	15		-2.03	Hybrid	15	10	-2.13
Joint hybrid	15	10	-2.00	LSTM	15		-2.1
Hybrid	15	10	-1.96	Hybrid	15	20	-2.07
Hybrid	15	20	-1.96	Hybrid	20	10	-2.05
Joint hybrid	20	10	-1.91	Joint hybrid	15	10	-2.03
LSTM	20		-1.88	LSTM	20		-2.03
Hybrid	20	10	-1.87	Hybrid	20	20	-2.02
Hybrid	20	20	-1.85	Joint hybrid	20	10	-1.97

(c) Single-patient Physionet data					(d) Multi-patient Physionet data				
Method	Features	LSTM dim	HMM states	LL	Method	Features	LSTM dim	HMM states	LL
HMM	Discretized		10	-0.68	Hybrid	Discretized	10	10	-0.61
LSTM	Continuous	5		-0.63	HMM	Discretized		10	-0.60
LSTM	Continuous	10		-0.63	Hybrid	Discretized	5	10	-0.59
Hybrid	Discretized	5	10	-0.39	LSTM	Discretized	10		-0.58
Hybrid	Discretized	10	10	-0.39	LSTM	Discretized	5		-0.56
LSTM	Discretized	5		-0.37	HMM	Continuous		10	-0.54
HMM	Continuous		10	-0.34	Hybrid	Continuous	5	10	-0.54
LSTM	Discretized	10		-0.33	Hybrid	Continuous	10	10	-0.54
Hybrid	Continuous	5	10	-0.33	LSTM	Continuous	5	10	-0.54
Hybrid	Continuous	10	10	-0.33	LSTM	Continuous	10	10	-0.54

and then add this information to the architecture in parallel with a 1-layer LSTM. The linear layer between the LSTM and the prediction layer is augmented with an extra column for each HMM state. The LSTM component of this architecture can be smaller than a standalone LSTM, since it only needs to fill in the gaps in the HMM’s predictions. The HMM is written in Python, and the rest of the architecture is in Torch.

We also build a joint hybrid model, where the LSTM and HMM are simultaneously trained in Torch, as shown in Figure 1b. We implemented an HMM Torch module, optimized using stochastic gradient descent rather than FFBS. Similarly to the sequential hybrid model, we concatenate the LSTM outputs with the HMM state probabilities.

3 Experiments

We test the methods on two text data sets used by Karpathy et al. (2016), Tiny Shakespeare (1M characters) and Linux Kernel (5M characters). We also use ICU medical data from the 2014 Physionet challenge, whose objective is to detect heart beat windows using 6 physiological signal features such as ECG measurements. We test on a single-patient data set with 200K time points, predicting future heart beats for the same patient, and a multi-patient data set with 15 training and 5 test patients.

```

- pm_qos_update_flags = Update a set of PM_QoS flags;
- @pm_qos_update_flags: To update
- @pm_qos_update_flags: To update
- @action: Action to take on the state
- @val: Value of the request to a _pm_qos_

- Update the given set of PM_QoS flags and call the
- will_change. Returns 1 if the given constraint
- is 0, otherwise.

bool pm_qos_update_flags(struct pm_qos_flags *pqr,
struct pm_qos_flags_request *rq,
enum pm_qos_request_action_t s_val)
{
    unsigned long irqflags;
    spin_lock_irqsave(&pm_qos_lock, irqflags);

    pqr->val = 1; if (!pqr->val) pqr->val = 0;

    switch (action) {
    case PM_QOS_REMOVE_REQ:
        pm_qos_flags_remove_req(pqr, rq);
        break;
    case PM_QOS_UPDATE_REQ:
        pm_qos_flags_update_req(pqr, rq);
        break;
    case PM_QOS_ADD_REQ:
        rq->flags = val;
        INIT_LIST_HEAD(&rq->node);
        list_add_tail(&rq->node, &pqr->list);
        pqr->flags |= val;
        break;
    default:
        /* do nothing */
    }
}

+ pm_qos_update_flags = Update a set of PM_QoS flags;
+ @pm_qos_update_flags: To update
+ @pm_qos_update_flags: To update
+ @action: Action to take on the state
+ @val: Value of the request to a _pm_qos_

+ Update the given set of PM_QoS flags and call the
+ will_change. Returns 1 if the given constraint
+ is 0, otherwise.

bool pm_qos_update_flags(struct pm_qos_flags *pqr,
struct pm_qos_flags_request *rq,
enum pm_qos_request_action_t s_val)
{
    unsigned long irqflags;
    spin_lock_irqsave(&pm_qos_lock, irqflags);

    pqr->val = 1; if (!pqr->val) pqr->val = 0;

    switch (action) {
    case PM_QOS_REMOVE_REQ:
        pm_qos_flags_remove_req(pqr, rq);
        break;
    case PM_QOS_UPDATE_REQ:
        pm_qos_flags_update_req(pqr, rq);
        break;
    case PM_QOS_ADD_REQ:
        rq->flags = val;
        INIT_LIST_HEAD(&rq->node);
        list_add_tail(&rq->node, &pqr->list);
        pqr->flags |= val;
        break;
    default:
        /* do nothing */
    }
}

```

(a) Hybrid HMM component: colors correspond to 10 HMM states. Distinguishes comments and indentation spaces (green, yellow font) from other spaces (purple). Red cluster (with yellow font) identifies punctuation and brackets. Green cluster (yellow font) also finds capitalized variable names.

(b) Hybrid LSTM component: colors correspond to 10 k-means clusters on hidden state vectors. Distinguishes comments, spaces at beginnings of lines, and spaces between words (red, white font) from indentation spaces (green, yellow font). Opening brackets are red (yellow font), closing brackets are green (white font).

Figure 2: Visualizing HMM and LSTM states on Linux data for the hybrid with 10 LSTM state dimensions and 10 HMM states. The HMM and LSTM components learn some complementary features in the text related to spaces and comments.

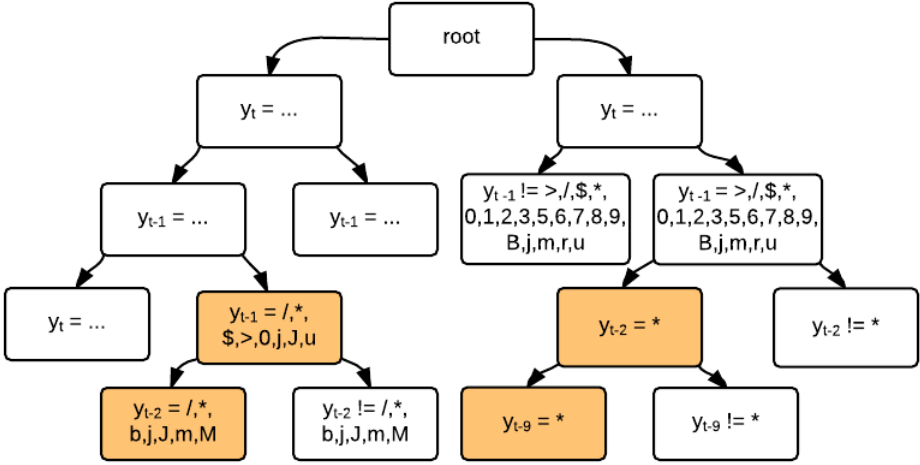


Figure 3: Decision tree predicting an individual hidden state dimension of the hybrid algorithm based on the preceding characters on the Linux data. Nodes with uninformative splits are represented with ...

For the text data sets, Tables 1a and 1b shows the predictive log likelihood for the next text character for each method. The sequential hybrid algorithm performs a bit better than the standalone LSTM with the same LSTM state dimension. This effect gets smaller as we increase the LSTM size and the HMM makes less difference to the prediction. The hybrid algorithm with 20 HMM states does better than the one with 10 HMM states. The joint hybrid algorithm outperforms the sequential hybrid on Shakespeare data, but does worse on Linux data, which suggests that the joint hybrid is more helpful for smaller data sets. The joint hybrid is an order of magnitude slower than the sequential hybrid, as the SGD-based HMM is slower to train than the FFBS-based HMM.

We interpret the HMM and LSTM states in the hybrid algorithm with 10 LSTM state dimensions and 10 HMM states in Figure 2, showing which text features are identified by the HMM and LSTM components for the Linux data. In Figure 2a, we color-code the training data with the 10 HMM states. In Figure 2b, we apply k-means clustering to the LSTM state vectors, and color-code the training data with the clusters. The HMM and LSTM states pick up on spaces, indentation, and special characters (such as comment symbols in Linux data). Sometimes, the HMM and LSTM complement each other, such as learning different features related to spaces and comments in the Linux data. In Figure 3, we see that some individual LSTM hidden state dimensions identify similar features, such as comment symbols in the Linux data. The 10 hidden state dimensions of the hybrid algorithm mostly track comment characters, which suggests these features have a distributed representation.

For the Physionet data, we try the methods on continuous features and discretized features. Tables 1c and 1d shows the predictive log likelihood for the heart beat indicator for each method. Curiously, discretizing the single-patient data makes the LSTM perform better, while the HMM and hybrid perform worse, with the hybrid on continuous features and LSTM of dimension 10 on discretized features performing the best. We do not observe this effect on the multi-patient data set, where all the methods perform better (and similarly) on continuous features. The LSTM dimension mostly doesn't matter for these data sets. The hybrid algorithm does not decrease the state dimension for the multi-patient data set, while the smaller single-patient data the hybrid of dimension 5 performs the same as the LSTM of dimension 10 without relying on discretization.

4 Conclusion

Hybrid HMM-RNN approaches combine the interpretability of HMMs with the predictive power of RNNs. A small hybrid model usually performs better than a standalone LSTM of the same size, especially on smaller data sets. We use visualizations to show how the LSTM and HMM components of the hybrid algorithm complement each other in terms of features learned in the data.

References

- Bourlard, H. and Morgan, N. (1994). *Connectionist Speech Recognition: A Hybrid Approach*. Kluwer Academic Publishers.
- Che, Z., Purushotham, S., and Liu, Y. (2015). Distilling Knowledge from Deep Networks with Applications to Healthcare Domain. *Neural Information Processing Systems Workshop on Machine Learning for Healthcare (MLHC)*.
- Karpathy, A., Johnson, J., and Fei-Fei, L. (2016). Visualizing and Understanding Recurrent Networks. *International Conference for Learning Representations Workshop Track*.
- Kim, B., Shah, J. A., and Doshi-Velez, F. (2015). Mind the Gap: A Generative Approach to Interpretable Feature Selection and Extraction. In Cortes, C., Lawrence, N. D., Lee, D. D., Sugiyama, M., and Garnett, R., editors, *Neural Information Processing Systems (NIPS)*, pages 2260–2268.
- Lipton, Z. C. (2016). The Mythos of Model Interpretability. *2016 ICML Workshop on Human Interpretability in Machine Learning (WHI)*, New York, NY.
- Maas, A., Le, Q., O’Neil, T., Vinyals, O., Nguyen, P., and Ng, A. (2012). Recurrent Neural Networks for Noise Reduction in Robust ASR. In *Proceedings of INTERSPEECH*.
- Rao, V. and Teh, Y. W. (2013). Fast MCMC sampling for Markov jump processes and extensions. *Journal of Machine Learning Research*, 14:3207–3232. arXiv:1208.4818.

Ribeiro, M. T., Singh, S., and Guestrin, C. (2016). "Why Should I Trust You?": Explaining the Predictions of Any Classifier. *CoRR*, abs/1602.04938.

Szegedy, C., Zaremba, W., Sutskever, I., Bruna, J., Erhan, D., Goodfellow, I., and Fergus, R. (2014). Intriguing properties of neural networks. In *International Conference on Learning Representations*.

Turner, R. (2016). A Model Explanation System: Latest Updates and Extensions. *2016 ICML Workshop on Human Interpretability in Machine Learning (WHI)*, New York, NY.